



Regular article

## Massive $\mathcal{N} = 2$ Supersymmetric Gauge Theory Under Electric Field Quench

Leila Shahkarami

School of Physics, Damghan University, Damghan, P.O.Box 36716-41167, Iran.  
E-mail: [l.shahkarami@du.ac.ir](mailto:l.shahkarami@du.ac.ir)

**Received:** February 21, 2024; **Revised:** March 15, 2024; **Accepted:** March 25, 2024

**Abstract.** This study investigates the non-equilibrium dynamics of massive  $\mathcal{N} = 2$  supersymmetric gauge theory under pulse-like electric field quenches, utilizing holographic techniques within the AdS/CFT correspondence framework. Focusing on subcritical electric fields, our analysis reveals prolonged oscillations in the electric current as well as the quark condensate dynamics with no dissipation. Notably, through power spectrum analysis of the time-dependent electric current, we identify a dominant frequency in the oscillations, which remains the same within numerical precision across different parameter variations, serving as a universal feature of the system.

*Keywords:* AdS/CFT Correspondence; Quantum Quench; Pulsed Electric Field.

---

**COPYRIGHTS:** ©20243, Journal of Holography Applications in Physics. Published by Damghan University. This article is an open-access article distributed under the terms and conditions of the Creative Commons Attribution 4.0 International (CC BY 4.0).

<https://creativecommons.org/licenses/by/4.0>



## 1 Introduction

The exploration of quantum vacuum response under strong external fields provides valuable insights into fundamental physical processes. One prominent phenomenon, known as the Sauter-Schwinger effect, elucidates the creation of electron-positron pairs from the vacuum in the presence of a constant homogeneous electric field [1]. This effect, initially studied in the context of quantum electrodynamics (QED), has broader implications, extending to gauge theories such as quantum chromodynamics (QCD), where quarks which are also charged particles introduce additional complexity.

Previous studies have primarily focused on constant electric fields, with limited applicability to real-world experimental conditions. However, recent research has underscored the importance of considering time- and even spatially-dependent electric fields to bridge the gap between theoretical predictions and experimental observations (see, e.g., [2, 3, 4, 5, 6, 7]). Such investigations moreover reveal critical insights into the non-equilibrium behavior of gauge theories, shedding light on phenomena inaccessible under equilibrium conditions.

Utilizing holographic techniques, particularly the AdS/CFT correspondence [8], offers a powerful framework for studying strongly-coupled gauge theories like QCD in regimes where traditional perturbative methods falter. This is especially important when dealing with phenomena like the Schwinger effect, which is inherently nonperturbative in nature. Previous work has primarily focused on exploring the holographic Schwinger effect within the context of constant electric fields (see, e.g., [9, 10, 11, 12, 13, 14, 15, 16, 17]). Among its important clarifications about both the Schwinger effect and the nonperturbative properties of strongly-coupled theories, the AdS/CFT duality has verified the existence of a critical electric field  $E_c$  (dependent on the particle masses), above which particle production from the vacuum occurs without any obstacle. There are also few works considering the impact of time-dependent electric fields on the system [12, 18, 19, 20, 21, 22, 23], that provided valuable insights into the real-time dynamics of gauge theories.

In [23], we employed the  $\mathcal{N} = 2$   $SU(N_c)$  supersymmetric gauge theory at zero temperature, focusing on its response to time-dependent electric fields with special configurations similar to a Gaussian pulse. Due to the assumption of massless quarks, the critical electric field was zero, resulting in the immediate generation of electric currents even for infinitesimally small applied electric fields. The study revealed intriguing phenomena, including the emergence of an oscillatory region resembling underdamped harmonic oscillatory pattern at the late-time behavior of the response electric current. We furthermore found a unique frequency for these oscillations regardless of the details of the pulse function and its parameters.

While this work shed light on the behavior of the system under pulse-like electric field quenches, it left several questions unanswered. The absence of quark masses precluded the exploration of scenarios where the maximum of the applied electric field falls below the critical threshold. Consequently, the response of the system to quenches with a maximum value lower than the critical electric field remained unexplored. Furthermore, the late-time underdamped oscillatory pattern observed in the electric current dynamics prompts further investigations into the influence of a mass gap on the problem. Additionally, there is motivation to explore the frequencies of the oscillations in the presence of massive quarks.

In the present study, we aim to address these outstanding questions by extending our investigation to include massive quarks in the same background as in [23], exposed to a time-dependent pulse-like external electric field. The inclusion of massive quarks reflects a more realistic scenario. By numerically solving the relevant equations derived from the D7 brane DBI action in the gravity side, we explore the dynamical evolution of the developed electric current in response to the pulse-like electric field. Introducing the quark mass

renders the quark condensation nontrivial anymore and its nontrivial dynamics should be obtained alongside that of the electric current. By studying the dynamics of both of these quantities, we aim to address some of the unresolved questions from the massless case and provide deeper insights into the non-equilibrium dynamics of supersymmetric  $SU(N_c)$  gauge theories.

The remainder of the paper is structured as follows: In the next section, we provide a brief introduction to the model and present the evolution equations obtained from the DBI action. We then describe the main aspects of the numerical technique used to solve these equations in Section 3. The resulting graphs are presented and analyzed in Section 4. Finally, in Section 5, we summarize our findings and discuss the main conclusions drawn from this study.

## 2 $\mathcal{N} = 2$ $SU(N_c)$ supersymmetric theory

We study the system considered in [23] but with a mass gap. Our aim is to explore the far-from-equilibrium dynamics of this system induced by a homogeneous but time-dependent electric field, which is turned on at an initial time and decreases again to zero after reaching a maximum value of  $E_m$ .

To construct our model, we embed a probe D7 brane into the  $AdS_5 \times S^5$  geometry to introduce the fundamental quarks on the gauge theory side. According to the AdS/CFT dictionary, this system corresponds to strongly-coupled  $\mathcal{N} = 2$   $SU(N_c)$  supersymmetric QCD at large  $N_c$  and at zero temperature. This toy model exhibits quark confinement only in the meson sector. Previous studies have shown that in the static case, a minimum value  $E_c$  of the electric field is required to break the confinement, resulting in a nonzero electric current of charged quarks. The value of the critical electric field  $E_c$  increases with the mass of the quarks ( $E_c = 0$  for massless quarks). Additionally, in static problems, the D7 brane solutions for subcritical and supercritical electric fields are described by Minkowski and black hole embeddings, respectively.

The metric of the  $AdS_5 \times S^5$  geometry is expressed as follows:

$$ds_{10}^2 = \frac{R^2}{z^2} (-dt^2 + d\vec{x}^2 + dz^2) + R^2 (d\phi^2 + \cos^2\phi d\Omega_3^2 + \sin^2\phi d\psi^2). \quad (1)$$

Here,  $R$  is the AdS radius and  $V$  represents the ingoing Eddington-Finkelstein coordinate, defined as  $dV = dt - dz$ .  $z$  denotes the radial bulk coordinate which is zero at the boundary. The dynamics of the D7 brane is described by the following Dirac-Born-Infeld (DBI) action:

$$S_{D7} = -\tau_7 \int d^8\sigma \sqrt{-\det [P(g)_{ab} + 2\pi\alpha' F_{ab}]}, \quad (2)$$

where  $P(g)_{ab}$  and  $F_{ab} = \partial_a A_b - \partial_b A_a$  are respectively the induced metric and the electromagnetic field strength tensor on the brane. Also,  $\tau_7 = (2\pi)^{-7} \alpha'^{-4} g_s^{-1}$ , where  $g_s$  denotes the string coupling and  $\alpha'$  is a string theory parameter so that  $1/(2\pi\alpha')$  is the string tension. Moreover,  $\sigma_a$  denote the brane worldvolume coordinates. To introduce an electric field along one of the spatial coordinates of the gauge theory, say  $x_1$ , we choose the gauge potential to be in the following form:

$$2\pi\alpha' R^{-2} A_a d\sigma^a = a(V, z) dx_1. \quad (3)$$

Notice that in this paper we focus on zero baryon number case. To study the effect of static fields (where  $a(V, z) \rightarrow -EV + a(z)$  where  $E$  is a constant electric field applied in

$x_1$  direction), one usually employs  $(V, z, \Omega_3, \vec{x}_3)$  as the worldvolume coordinates of the D7 brane. Thus, the shape of the D7 brane in the bulk is determined by the functionality of the other two perpendicular coordinates of the gravity side, i.e.,  $\phi$  and  $\psi$ . Since one can set  $\psi = 0$  utilizing the  $U(1)$  symmetry, the brane solutions are determined by  $\phi(z)$ .

The absence of a mass gap corresponds to a flat probe D7 brane configuration in the bulk geometry where the D7 brane touches the stack of  $N_c$  D3-branes. In such a case, similar to the one considered in [23],  $\phi$  can simply be chosen to be zero. However, in the present paper, where the quarks are supposed to be massive, the functionality of  $\phi$  needs to be determined along with  $a$  by solving the coupled equations of motion.

It is important to note that in our problem, both the gauge field and  $\phi$  would be functions of time  $V$  and radial coordinate  $z$ . To follow the numerical strategy proposed in [18, 24] for solving such problems, we use  $(\Omega_3, \vec{x}_3)$  for six of the worldvolume coordinates of the D7 brane. For the other two coordinates, we introduce a double-null coordinate system  $(u, v)$  instead of the target space coordinates  $(V, z)$ , which are used in the static case. Therefore, the dynamical variables are

$$V = V(u, v), \quad z = Z(u, v), \quad \phi = \Phi(u, v), \quad \psi = 0, \quad a = a(u, v). \quad (4)$$

Substituting the induced metric and the above relations into (2), we arrive at

$$S_{D7} = -2\pi^2 \tau_7 V_3 \int dudv \frac{\cos^3 \Phi}{Z^3} \sqrt{\xi},$$

$$\xi = (g_{uv} + Z^2 \partial_u a \partial_v a)^2 - (g_{uu} + Z^2 \partial_u a^2) (g_{vv} + Z^2 \partial_v a^2), \quad (5)$$

where  $V_3$  is the volume of the spatial coordinates of the field theory, and

$$g_{uv} = -Z^{-2} (V_{,u} V_{,v} + V_{,u} Z_{,v} + V_{,v} Z_{,u}) + \Phi_{,u} \Phi_{,v},$$

$$g_{uu} = -Z^{-2} V_{,u} (V_{,u} + 2Z_{,u}) + \Phi_{,u}^2, \quad g_{vv} = -Z^{-2} V_{,v} (V_{,v} + 2Z_{,v}) + \Phi_{,v}^2. \quad (6)$$

One can leverage the freedom in coordinates  $(u, v)$  to simplify the Dirac-Born-Infeld (DBI) action. To achieve this, we impose the following coordinate conditions as constraint equations:

$$g_{uu} + Z^2 (\partial_u a)^2 = 0,$$

$$g_{vv} + Z^2 (\partial_v a)^2 = 0. \quad (7)$$

Under these double-null conditions, the square root in the DBI action can be eliminated, simplifying the action to

$$S_{D7} = -2\pi^2 \tau_7 V_3 \int dudv \frac{\cos^3 \Phi}{Z^3} (g_{uv} + Z^2 \partial_u a \partial_v a). \quad (8)$$

Varying this action, one finds the following coupled evolution equations:

$$V_{,uv} = \frac{3}{2}Z(Z\Psi)_{,u}(Z\Psi)_{,v} + \frac{3}{2}\tan(Z\Psi)[(Z\Psi)_{,u}V_{,v} + (Z\Psi)_{,v}V_{,u}] - \frac{5}{2Z}V_{,u}V_{,v} + \frac{Z^3}{2}a_{,u}a_{,v}, \quad (9)$$

$$Z_{,uv} = -\frac{3}{2}Z(Z\Psi)_{,u}(Z\Psi)_{,v} + \frac{3}{2}\tan(Z\Psi)[(Z\Psi)_{,u}Z_{,v} + (Z\Psi)_{,v}Z_{,u}] + \frac{5}{Z}Z_{,u}Z_{,v} - \frac{Z^3}{2}a_{,u}a_{,v} + \frac{5}{2Z}(V_{,u}V_{,v} + V_{,u}Z_{,v} + V_{,v}Z_{,u}), \quad (10)$$

$$\begin{aligned} \Psi_{,uv} = & \frac{3}{2}\left(\Psi + \frac{\tan(Z\Psi)}{Z}\right)(Z\Psi)_{,u}(Z\Psi)_{,v} + \frac{1 - 3Z\Psi\tan(Z\Psi)}{2Z^2}[(Z\Psi)_{,u}Z_{,v} + (Z\Psi)_{,v}Z_{,u}] \\ & - \frac{\Psi}{2Z^2}\left(5 - \frac{3\tan(Z\Psi)}{Z\Psi}\right)(V_{,u}V_{,v} + V_{,u}Z_{,v} + V_{,v}Z_{,u}) + \frac{Z^2\Psi}{2}\left(1 - \frac{3\tan(Z\Psi)}{Z\Psi}\right)a_{,u}a_{,v} \\ & - \frac{3\Psi}{Z^2}Z_{,u}Z_{,v}, \end{aligned} \quad (11)$$

$$a_{,uv} = \frac{3}{2}\tan(Z\Psi)[(Z\Psi)_{,u}a_{,v} + (Z\Psi)_{,v}a_{,u}] + \frac{1}{2Z}(Z_{,u}a_{,v} + Z_{,v}a_{,u}), \quad (12)$$

where  $\Psi(u, v) = \frac{\Phi(u, v)}{Z(u, v)}$  is a variable used instead of  $\Phi(u, v)$ .

We will employ the numerical method initially developed in [24] and later utilized in [18, 25, 22] to solve this set of differential equations. Details of the method can be found in [24]. Here, we only briefly mention the required initial and boundary conditions.

## 2.1 Near boundary expansions

Solving Eqs. (9-12), one can determine  $a$  and  $\Psi$  as functions of  $V$  and  $Z$ . All the essential physical quantities can be obtained by expanding these functions near the AdS boundary  $Z = 0$ , yielding:

$$\Psi(V, Z) = m + \left(c(V) + \frac{m^3}{6}\right)Z^2 + \dots, \quad (13)$$

$$a(V, Z) = \alpha_0(V) + \dot{\alpha}_0(V)Z + \frac{1}{2}J(V)Z^2 + \frac{1}{2}\ddot{\alpha}_0(V)Z^2 \ln(mZ) + \dots \quad (14)$$

In the expansion of the scalar field  $\Psi$ ,  $m$  and  $c(V)$  are respectively related to the quark mass and quark condensate in the gauge theory. Moreover, the leading term in the second expansion is related to the applied electric field in the field theory and can be expressed as:

$$\alpha_0(V) = -\int^V dV' E(V'). \quad (15)$$

In this paper, we choose the following form for the time-dependent electric field:

$$E(V) = E_m \begin{cases} 0, & V < 0, \\ \cos^2\left(\frac{\pi V}{2\delta t} + \frac{\pi}{2}\right), & 0 \leq V \leq 2\delta t, \\ 0, & V > 2\delta t, \end{cases} \quad (16)$$

where  $E_m$  is the maximum value of the electric field and  $\delta t$  is the ramping time. Furthermore,  $J(V)$  represents the dynamical electric current in the boundary theory.

Once the source terms are provided by determining  $m$  and  $E(V)$ , the quark condensate  $c(V)$  and electric current  $J(V)$  can be obtained as the response of the gauge theory through solving the evolution equations in the bulk. We set  $m = 1$  for simplicity in the subsequent analysis and results. In the next section, we investigate the effect of a typical pulse-like electric field like (16) using the graphs of  $c(V)$  and  $J(V)$  obtained from the numerical calculations. Before proceeding, we present the conditions on the variables required for solving Eqs. (9-12) and provide a brief review of the numerical methods.

## 2.2 Numerical technique

In our study, we utilize numerical techniques to explore the time evolution of the D7 brane. We adopt the numerical approach outlined in [24] for determining the probe D7 brane solutions under dynamic conditions. To facilitate this, we transit to double-null coordinates, denoted as  $u$  and  $v$ , replacing the  $(V, z)$  coordinates. Subsequently, upon applying the coordinate conditions (7) to the evolution equations, we obtain a coupled set of differential equations governing the functions  $Z(u, v)$ ,  $V(u, v)$ ,  $\Psi(u, v)$ , and  $a(u, v)$ . The numerical strategy described in [24] distinguishes between two different schemes based on whether the brane intersects with the event horizon or not. In our case, we focus on Minkowski solutions, where the maximum electric field remains sufficiently below the critical electric field. Consequently, we provide a brief overview of the corresponding numerical scheme applicable before the brane intersects with the event horizon.

To solve Eqs. (9-12), we employ the finite difference method in the  $u$ - $v$  plane. The imposition of constraints (7) ensures numerical stability. Using coordinate freedom, we fix the location of the AdS boundary  $Z = 0$  and the pole  $\Phi = \pi/2$  at  $u = v$  and  $u = v + \pi/2$ , respectively.

Applying the asymptotic behavior of the quantities in Eqs. (13) and (14), we derive boundary conditions at the AdS boundary, expressed as:

$$Z|_{u=v} = 0, \quad \Psi|_{u=v} = m, \quad a|_{u=v} = \alpha_0(V), \quad V_v|_{u=v} = 2Z_u|_{u=v}. \quad (17)$$

Here, the condition for  $V$  is determined by ensuring the regularity of the evolution equation near the AdS boundary to satisfy the constraints.

Utilizing the regularities of the evolution equations at the pole, we express the conditions at the pole as:

$$(Z\Psi)|_{u=v+\pi/2} = \pi/2, \quad V_{,u} = V_{,v}, \quad Z_{,u} = Z_{,v}, \quad a_{,u} = a_{,v}. \quad (18)$$

Now, let us discuss the initial data. We select  $v = 0$  as the initial surface. The initial data for  $V < 0$ , corresponding to the pre-electric field activation stage, is obtained from the exact solution of the static embedding in pure AdS, given by:

$$\begin{aligned} V(u, 0) &= m^{-1}(u - \sin(u)) + V_{\text{ini}}, & Z(u, 0) &= m^{-1} \sin(u), \\ \Psi(u, 0) &= \frac{m u}{\sin(u)}, & a(u, 0) &= 0, \end{aligned} \quad (19)$$

where  $V_{\text{ini}}$  is an integration constant.

## 3 Results

This section presents the graphical outcomes derived from our numerical computations. Our focus lies on the behavior under subcritical electric fields, where the maximum electric field

value,  $E_m$ , remains significantly lower than the critical electric field. Notably, previous thermodynamic analyses in [26, 27] identified a first-order phase transition at  $E_c = 0.57588 m^2$ . This critical threshold has been validated through numerical calculations involving static electric fields applied to the present system holographically. For simplicity, we set  $m = 1$  throughout our results, maintaining generality.

Consistent with prior studies and affirmed by our calculations, when  $E_m$  remains notably below  $E_c$ , the D7 brane solution chooses the Minkowski embedding despite the system's dynamic nature.

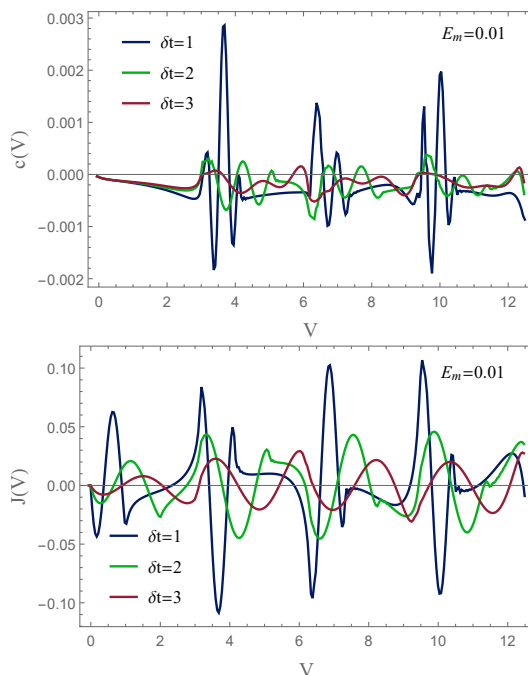


Figure 1: Time evolution of quark condensate  $c(V)$  and electric current  $J(V)$  for  $E_m = 0.01$  and  $\delta t = 1, 2, 3$ .

Figures 1 and 2 illustrate the quark condensate (left graphs) and electric current (right graphs) plotted against boundary time. In Fig. 1, we fix the maximum electric field value  $E_m$ , allowing observation of the impact of varying the ramping time  $\delta t$  on the system's dynamic response to the quench. Conversely, in Fig. 2 with fixed  $\delta t$ , we explore the effect of altering  $E_m$  by comparing the results.

Both figures reveal that upon turning on the electric field, both the electric current and quark condensate initiate oscillations, a phenomenon absent in the static case where a subcritical constant electric field yields a zero electric current. These oscillations, arising from the problem's dynamic nature, correspond to bound state oscillations of quarks in the field theory side. Notably, these oscillations persist over time, as demonstrated in Fig. 3, showcasing a long-term evolution of the electric current for a typical set of parameters. The preservation of oscillations over time is due to the fact that we have added the brane in the probe limit and neglected the bulk back reaction. This leads to conservation of the D7 brane's energy.

An interesting finding from Fig. 1 is that longer ramping times boost the oscillation strength. This aligns with other studies using tanh-like electric field profiles, where the

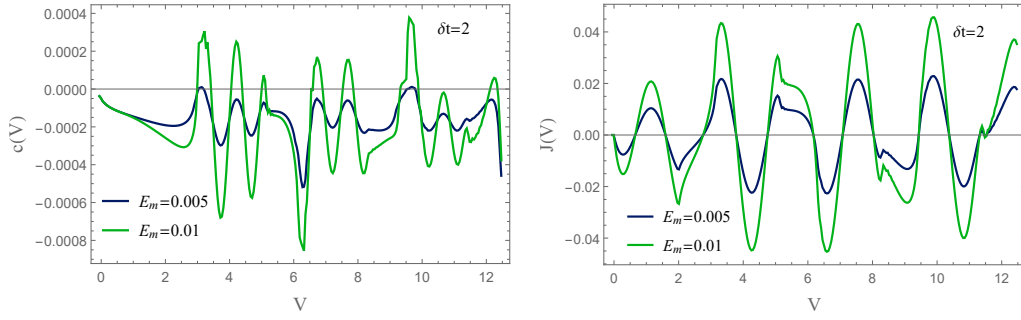


Figure 2: Time evolution of quark condensate  $c(V)$  and electric current  $J(V)$  for  $\delta t = 2$  and  $E_m = 0.005, 0.01$ .

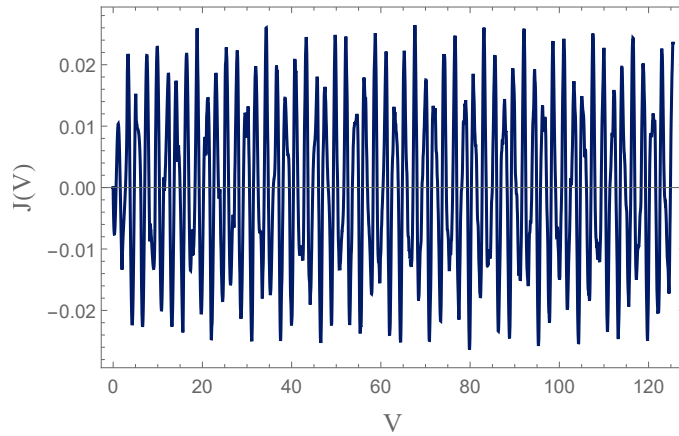


Figure 3: Long-term evolution of the electric current as a response to an electric pulse with parameters  $E_m = 0.005$  and  $\delta t = 2$ .

field gradually increases to a final finite value. However, our previous work ([23]) noted a different trend with pulse-like electric fields, where increasing ramping times decreases the amplitude of the oscillations for short enough ramping times. Exploring the effect of various ramping times in our current study, containing massive quarks, could provide valuable insights. Additionally, Fig. 2 indicates that oscillation amplitudes rise with  $E_m$ , as expected. Another intriguing observation is that oscillation patterns for both  $c$  and  $J$  synchronize when  $\delta t$  remains constant, i.e., the time courses are the same for various values of  $E_m$ , similar to what we observed in the massless case.

Lastly, analyzing the power spectrum helps identify key oscillation modes. Fig. 4 displays the frequency content of  $J(V)$  for different  $E_m$  values. Remarkably, regardless of the quenched electric field parameters, the first peak consistently occurs around  $\omega \approx 2.8$ . This frequency, showing the dominant oscillation mode of the D7 brane, is in fact a nonlinear counterpart of a normal mode seen in linear perturbations, remaining unchanged by altering the quench parameters within our numerical precision. This mode signifies the excitation of mesons within the field theory side. It is important to note that despite the presence of the electric field, these mesons remain stable, indicating that the field is not strong enough to melt them.

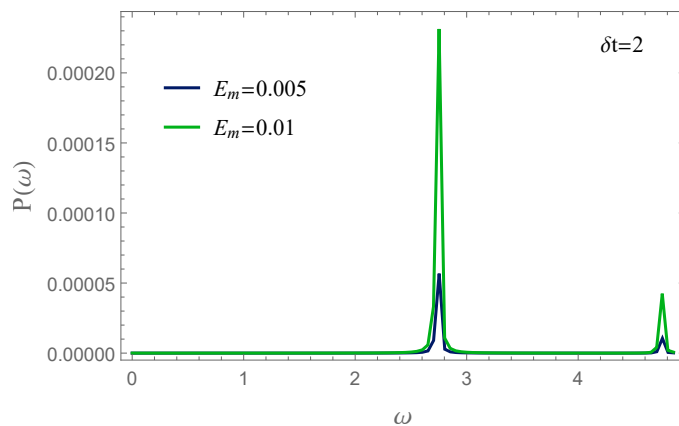


Figure 4: The power spectrum of  $J(V)$  for two electric pulses with parameters  $\delta t = 2$  and  $E_m = 0.005, 0.01$ .

## 4 Conclusion

In this study, we have investigated the far-from-equilibrium dynamics of a system similar to supersymmetric  $SU(N_c)$  gauge theories with massive quarks under the influence of time-dependent electric fields, employing holographic techniques within the framework of the AdS/CFT correspondence. Our investigation has aimed to provide insights into the behavior of strongly-coupled gauge theories, particularly in scenarios involving nonperturbative phenomena like the Schwinger effect.

Building upon our previous work [23], we have extended our analysis to include massive quarks, reflecting a more realistic representation of the system. This distinction is critical, as the presence of a mass gap introduces complexities in calculations which are not present in the massless case. Unlike previous calculation where the D7 brane's shape was fixed due to its intersection with the Poincare horizon, in the present scenario, the dynamics necessitate complicated numerical techniques. Specifically, we have utilized double-null coordinates and the finite difference method introduced in [24] to tackle the resulting differential equations.

Through numerical calculations derived from the D7 brane DBI action, we have explored the dynamic evolution of the system's electric current in response to pulse-like electric fields. We have focused on subcritical electric fields in this work. Our findings revealed intriguing phenomena, including the emergence of oscillatory patterns in both the electric current and quark condensate upon turning on the electric field. These oscillations persisted over time, reflecting the conservation of energy in the D7 brane, since here we are neglecting the bulk back reaction and the solution for the brane is the Minkowski embedding.

Furthermore, our study highlighted the influence of varying pulse parameters, i.e., the ramping time and maximum electric field value on the system's dynamics. Notably, we observed enhanced oscillation amplitudes with increasing ramping time and synchronized oscillation time courses for fixed ramping time values and different values of the maximum electric field.

Additionally, power spectrum analysis of the electric current shows that the dominant frequency is unique irrespective of the parameters of the quenched electric field pulse, and regarding the persistence of the oscillations over time without damping, this frequency is a nonlinear counterpart of a normal mode in linear perturbations.

In summary, our investigation offers deeper insights into the non-equilibrium dynamics

of supersymmetric  $SU(N_c)$  gauge theories, underscoring the importance of considering mass gaps and dynamic electric field scenarios. As future directions, it would be interesting to extend the present calculations to explore supercritical and near-critical electric fields. This would enable the study of thermalization and deconfinement processes under pulsed electric fields.

## Data Availability

The manuscript has no associated data.

## Conflicts of Interest

The author declares that there is no conflict of interest.

## Ethical Considerations

The author has diligently addressed ethical concerns, such as informed consent, plagiarism, data fabrication, misconduct, falsification, double publication, redundancy, submission, and other related matters.

## Funding

This research did not receive any grant from funding agencies in the public, commercial, or non-profit sectors.

## References

- [1] J. S. Schwinger, "On gauge invariance and vacuum polarization," *Phys. Rev.* **82**, 664 (1951). DOI: 10.1103/PhysRev.82.664
- [2] R. Schützhold, H. Gies, and G. Dunne, "Dynamically assisted Schwinger mechanism," *Phys. Rev. Lett.* **101**, 130404 (2008). DOI: 10.1103/PhysRevLett.101.130404
- [3] C. K. Dumlu, "Quantum kinetic approach and the scattering approach to vacuum pair production," *Phys. Rev. D* **179**, 065027 (2009). DOI: 10.1103/PhysRevD.79.065027
- [4] H. Gies and G. Torgrimsson, "Critical Schwinger pair production," *Phys. Rev. Lett.* **116**, 090406 (2016). DOI: 10.1103/PhysRevLett.116.090406
- [5] C. Schneider and R. Schützhold, "Dynamically assisted Sauter-Schwinger effect in inhomogeneous electric fields," *JHEP* **102**, 164 (2016). DOI: 10.1007/JHEP02(2016)164
- [6] A. Otto, D. Graeveling, and B. Kämpfer, "Response of the QED(2) vacuum to a quench: Long-term oscillations of the electric field and the pair creation rate," *Plasma Phys. Control. Fusion* **61**, 074002 (2019). DOI: 10.1088/1361-6587/ab1a21
- [7] I. A. Aleksandrov and C. Kohlfürst, "Pair production in temporally and spatially oscillating fields," *Phys. Rev. D* **101**, 096009 (2020). DOI: 10.1103/PhysRevD.101.096009

- [8] J. Maldacena, “The Large N limit of superconformal field theories and supergravity”, *Int. J. Theor. Phys.* **38**, 1113 (1999). DOI: 10.1023/A:1026654312961
- [9] G. W. Semenoff and K. Zarembo, “Holographic Schwinger effect,” *Phys. Rev. Lett.* **107**, 171601 (2011). DOI: 10.1103/PhysRevLett.107.171601
- [10] Y. Sato and K. Yoshida, “Potential analysis in holographic Schwinger effect,” *JHEP* **08**, 002 (2013). DOI: 10.1007/JHEP08(2013)002
- [11] S. Bolognesi, F. Kiefer, and E. Rabinovici, “Comments on critical electric and magnetic fields from holography,” *JHEP* **01**, 174 (2013). DOI: 10.1007/JHEP01(2013)174
- [12] K. Hashimoto and T. Oka, “Vacuum instability in electric fields via AdS/CFT: Euler-Heisenberg Lagrangian and Planckian thermalization,” *JHEP* **10**, 116 (2013). DOI: 10.1007/JHEP10(2013)116
- [13] Y. Sato and K. Yoshida, “Holographic Schwinger effect in confining phase,” *JHEP* **09**, 134 (2013). DOI: 10.1007/JHEP09(2013)134
- [14] J. Sadeghi, B. Pourhassan, S. Tahery, and F. Razavi, “Holographic Schwinger effect with a deformed AdS background,” *Int. J. Mod. Phys. A* **32**, 1750045 (2017). DOI: 10.1142/S0217751X17500452
- [15] L. Shahkarami, M. Dehghani, and P. Dehghani, “Holographic Schwinger effect in a D-instanton background,” *Phys. Rev. D* **97**, 046013 (2018). DOI: 10.1103/PhysRevD.97.046013
- [16] L. Shahkarami and F. Charmchi, “Confining D-instanton background in an external electric field,” *Eur. Phys. J. C* **79**, 343 (2019). DOI: 10.1140/epjc/s10052-019-6765-9
- [17] Sw. Li, Sk. Luo, and Hq. Li, “Holographic Schwinger effect and electric instability with anisotropy,” *JHEP* **08**, 206 (2022). DOI: 10.1007/JHEP08(2022)206
- [18] K. Hashimoto, S. Kinoshita, K. Murata, and T. Oka, “Electric field quench in AdS/CFT,” *JHEP* **09**, 126 (2014). DOI: 10.1007/JHEP09(2014)126
- [19] S. Amiri-Sharifi, M. Ali-Akbari, and H. R. Sepangi, “Electric field quench, equilibration and universal behavior,” *Phys. Rev. D* **91**, 126007 (2015). DOI: 10.1103/PhysRevD.91.126007
- [20] M. Ali-Akbari, H. Ebrahim, and S. Heshmatian, “Thermal quench at finite t’Hooft coupling,” *Nucl. Phys.* **B904**, 527 (2016). DOI: 10.1016/j.nuclphysb.2016.02.003
- [21] S. Amiri-Sharifi, M. Ali-Akbari, A. Kishani-Farahani, and N. Shafie, “Double relaxation via AdS/CFT,” *Nucl. Phys.* **B909**, 778 (2016). DOI: 10.1016/j.nuclphysb.2016.06.011
- [22] M. Ali-Akbari and F. Charmchi, “Holographic equilibration under external dynamical electric field,” *Phys. Lett. B* **773**, 271 (2017). DOI: 10.1016/j.physletb.2017.08.040
- [23] L. Shahkarami and F. Charmchi, “Late time oscillations and universal behavior in pulsed electric fields,” [arXiv:2308.02218 [hep-th]]. DOI: 10.48550/arXiv.2308.02218
- [24] T. Ishii, S. Kinoshita, K. Murata, and N. Tanahashi, “Dynamical meson melting in holography,” *JHEP* **04**, 099 (2014). DOI: 10.1007/JHEP04(2014)099

- [25] M. Ali-Akbari, F. Charmchi, A. Davody, H. Ebrahim, and L. Shahkarami, “Time-dependent meson melting in external magnetic field,” *Phys. Rev. D* **91**, 106008 (2015). DOI: 10.1103/PhysRevD.91.106008
- [26] T. Albash, V. G. Filev, C. V. Johnson, and A. Kundu, “Quarks in an external electric field in finite temperature large-N gauge theory,” *JHEP* **08**, 092 (2008). DOI: 10.1088/1126-6708/2008/08/092
- [27] J. Erdmenger, R. Meyer, and J. P. Shock, “AdS/CFT with flavour in electric and magnetic Kalb-Ramond fields,” *JHEP* **12**, 091 (2007). DOI: 10.1088/1126-6708/2007/12/091